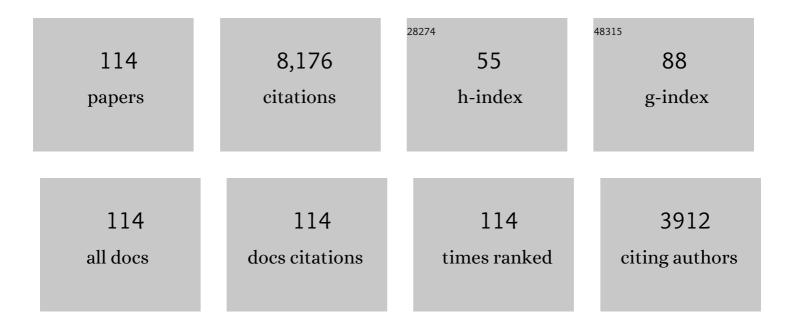
List of Publications by Year in descending order

Source: https://exaly.com/author-pdf/7493193/publications.pdf Version: 2024-02-01



HALLONGL

#	Article	IF	CITATIONS
1	An overview on engineering the surface area and porosity of biochar. Science of the Total Environment, 2021, 763, 144204.	8.0	434
2	CeO <sub>2</sub> –TiO <sub>2</sub> Catalysts for Catalytic Oxidation of Elemental Mercury in Low-Rank Coal Combustion Flue Gas. Environmental Science & Technology, 2011, 45, 7394-7400.	10.0	341
3	Superior activity of MnOx-CeO2/TiO2 catalyst for catalytic oxidation of elemental mercury at low flue gas temperatures. Applied Catalysis B: Environmental, 2012, 111-112, 381-388.	20.2	275
4	Development of Nano-Sulfide Sorbent for Efficient Removal of Elemental Mercury from Coal Combustion Fuel Gas. Environmental Science & Technology, 2016, 50, 9551-9557.	10.0	239
5	Mechanisms of peroxymonosulfate pretreatment enhancing production of short-chain fatty acids from waste activated sludge. Water Research, 2019, 148, 239-249.	11.3	188
6	Oxidation and capture of elemental mercury over SiO2–TiO2–V2O5 catalysts in simulated low-rank coal combustion flue gas. Chemical Engineering Journal, 2011, 169, 186-193.	12.7	185
7	The underlying mechanism of calcium peroxide pretreatment enhancing methane production from anaerobic digestion of waste activated sludge. Water Research, 2019, 164, 114934.	11.3	184
8	Role of flue gas components in mercury oxidation over TiO2 supported MnOx-CeO2 mixed-oxide at low temperature. Journal of Hazardous Materials, 2012, 243, 117-123.	12.4	174
9	Nitrogen in bio-oil produced from hydrothermal liquefaction of biomass: A review. Chemical Engineering Journal, 2020, 401, 126030.	12.7	165
10	Unveiling the mechanisms of how cationic polyacrylamide affects short-chain fatty acids accumulation during long-term anaerobic fermentation of waste activated sludge. Water Research, 2019, 155, 142-151.	11.3	159
11	Understanding and mitigating the toxicity of cadmium to the anaerobic fermentation of waste activated sludge. Water Research, 2017, 124, 269-279.	11.3	157
12	SCR Atmosphere Induced Reduction of Oxidized Mercury over CuO–CeO <sub>2</sub> /TiO <sub>2</sub> Catalyst. Environmental Science & Technology, 2015, 49, 7373-7379.	10.0	153
13	Triclocarban enhances short-chain fatty acids production from anaerobic fermentation of waste activated sludge. Water Research, 2017, 127, 150-161.	11.3	150
14	Fe(II) catalyzing sodium percarbonate facilitates the dewaterability of waste activated sludge: Performance, mechanism, and implication. Water Research, 2020, 174, 115626.	11.3	150
15	CO2 capture by Li4SiO4 sorbents and their applications: Current developments and new trends. Chemical Engineering Journal, 2019, 359, 604-625.	12.7	142
16	Magnetic iron–manganese binary oxide supported on carbon nanofiber (Fe3â^'xMnxO4/CNF) for efficient removal of HgO from coal combustion flue gas. Chemical Engineering Journal, 2018, 334, 216-224.	12.7	135
17	Selenium Functionalized Metal–Organic Framework MIL-101 for Efficient and Permanent Sequestration of Mercury. Environmental Science & Technology, 2019, 53, 2260-2268.	10.0	133
18	Progress in MgO sorbents for cyclic CO <sub>2</sub> capture: a comprehensive review. Journal of Materials Chemistry A, 2019, 7, 20103-20120.	10.3	132

#	Article	IF	CITATIONS
19	A review on pyrolysis of protein-rich biomass: Nitrogen transformation. Bioresource Technology, 2020, 315, 123801.	9.6	131
20	Multiform Sulfur Adsorption Centers and Copper-Terminated Active Sites of Nano-CuS for Efficient Elemental Mercury Capture from Coal Combustion Flue Gas. Langmuir, 2018, 34, 8739-8749.	3.5	128
21	Sulfur abundant S/FeS2 for efficient removal of mercury from coal-fired power plants. Fuel, 2018, 232, 476-484.	6.4	126
22	Impact of SO2 on elemental mercury oxidation over CeO2–TiO2 catalyst. Chemical Engineering Journal, 2013, 219, 319-326.	12.7	125
23	How does zero valent iron activating peroxydisulfate improve the dewatering of anaerobically digested sludge?. Water Research, 2019, 163, 114912.	11.3	124
24	Effects of thermal pretreatment on the biomethane yield and hydrolysis rate of kitchen waste. Applied Energy, 2016, 172, 47-58.	10.1	121
25	Simultaneous removal of SO2, NO and mercury using TiO2-aluminum silicate fiber by photocatalysis. Chemical Engineering Journal, 2012, 192, 21-28.	12.7	113
26	A review on nitrogen transformation in hydrochar during hydrothermal carbonization of biomass containing nitrogen. Science of the Total Environment, 2021, 756, 143679.	8.0	108
27	Fabrication of Heterostructured g-C3N4/Ag-TiO2 Hybrid Photocatalyst with Enhanced Performance in Photocatalytic Conversion of CO2 Under Simulated Sunlight Irradiation. Applied Surface Science, 2017, 402, 198-207.	6.1	104
28	Magnetic Rattle-Type Fe <sub>3</sub> O <sub>4</sub> @CuS Nanoparticles as Recyclable Sorbents for Mercury Capture from Coal Combustion Flue Gas. ACS Applied Nano Materials, 2018, 1, 4726-4736.	5.0	100
29	In Situ Decoration of Selenide on Copper Foam for the Efficient Immobilization of Gaseous Elemental Mercury. Environmental Science & Technology, 2020, 54, 2022-2030.	10.0	96
30	CuO–CeO <sub>2</sub> /TiO <sub>2</sub> catalyst for simultaneous NO reduction and Hg <sup>0</sup> oxidation at low temperatures. Catalysis Science and Technology, 2015, 5, 5129-5138.	4.1	95
31	Incorporation of CaO into inert supports for enhanced CO2 capture: A review. Chemical Engineering Journal, 2020, 396, 125253.	12.7	92
32	Enhanced short-chain fatty acids production from waste activated sludge by sophorolipid: Performance, mechanism, and implication. Bioresource Technology, 2019, 284, 456-465.	9.6	91
33	Machine learning prediction and optimization of bio-oil production from hydrothermal liquefaction of algae. Bioresource Technology, 2021, 342, 126011.	9.6	82
34	Synergy of CuO and CeO2 combination for mercury oxidation under low-temperature selective catalytic reduction atmosphere. International Journal of Coal Geology, 2017, 170, 69-76.	5.0	77
35	Kinetics of mercury oxidation in the presence of hydrochloric acid and oxygen over a commercial SCR catalyst. Chemical Engineering Journal, 2013, 220, 53-60.	12.7	76
36	Effect of Nitrogen Oxides on Elemental Mercury Removal by Nanosized Mineral Sulfide. Environmental Science & Technology, 2017, 51, 8530-8536.	10.0	75

#	Article	IF	CITATIONS
37	Nanosized Copper Selenide Functionalized Zeolitic Imidazolate Frameworkâ€8 (CuSe/ZIFâ€8) for Efficient Immobilization of Gasâ€Phase Elemental Mercury. Advanced Functional Materials, 2019, 29, 1807191.	14.9	74
38	Promotional effect of CuO loading on the catalytic activity and SO2 resistance of MnOx/TiO2 catalyst for simultaneous NO reduction and Hg0 oxidation. Fuel, 2018, 227, 79-88.	6.4	73
39	Enhanced Short-Chain Fatty Acids from Waste Activated Sludge by Heat–CaO <sub>2</sub> Advanced Thermal Hydrolysis Pretreatment: Parameter Optimization, Mechanisms, and Implications. ACS Sustainable Chemistry and Engineering, 2019, 7, 3544-3555.	6.7	71
40	Removal of elemental mercury from flue gas by recyclable CuCl2 modified magnetospheres from fly ash. Part 4. Performance of sorbent injection in an entrained flow reactor system. Fuel, 2018, 220, 403-411.	6.4	70
41	Activation of Persulfates Using Siderite as a Source of Ferrous Ions: Sulfate Radical Production, Stoichiometric Efficiency, and Implications. ACS Sustainable Chemistry and Engineering, 2018, 6, 3624-3631.	6.7	67
42	One-step synthesis of spherical CaO pellets via novel graphite-casting method for cyclic CO2 capture. Chemical Engineering Journal, 2019, 374, 619-625.	12.7	65
43	Heat pretreatment assists free ammonia to enhance hydrogen production from waste activated sludge. Bioresource Technology, 2019, 283, 316-325.	9.6	65
44	Copper slag as a catalyst for mercury oxidation in coal combustion flue gas. Waste Management, 2018, 74, 253-259.	7.4	64
45	Mechanisms of potassium permanganate pretreatment improving anaerobic fermentation performance of waste activated sludge. Chemical Engineering Journal, 2021, 406, 126797.	12.7	64
46	Removal of Gas-Phase Elemental Mercury in Flue Gas by Inorganic Chemically Promoted Natural Mineral Sorbents. Industrial & Engineering Chemistry Research, 2012, 51, 3039-3047.	3.7	63
47	Bioenergy recovery from wastewater produced by hydrothermal processing biomass: Progress, challenges, and opportunities. Science of the Total Environment, 2020, 748, 142383.	8.0	63
48	Surface-Engineered Sponge Decorated with Copper Selenide for Highly Efficient Gas-Phase Mercury Immobilization. Environmental Science & Technology, 2020, 54, 16195-16203.	10.0	63
49	Electrospun metal oxide–TiO2 nanofibers for elemental mercury removal from flue gas. Journal of Hazardous Materials, 2012, 227-228, 427-435.	12.4	62
50	Elemental mercury oxidation over manganese oxide octahedral molecular sieve catalyst at low flue gas temperature. Chemical Engineering Journal, 2019, 356, 142-150.	12.7	62
51	Binding of Mercury Species and Typical Flue Gas Components on ZnS(110). Energy & Fuels, 2017, 31, 5355-5362.	5.1	60
52	Mercury Removal from Flue Gas by Noncarbon Sorbents. Energy & Fuels, 2021, 35, 3581-3610.	5.1	60
53	Role of Sulfur Trioxide (SO <sub>3</sub> ) in Gas-Phase Elemental Mercury Immobilization by Mineral Sulfide. Environmental Science & Technology, 2019, 53, 3250-3257.	10.0	58
54	Cobalt doped ceria for abundant storage of surface active oxygen and efficient elemental mercury oxidation in coal combustion flue gas. Applied Catalysis B: Environmental, 2018, 239, 233-244.	20.2	57

#	Article	IF	CITATIONS
55	Amorphous Molybdenum Selenide Nanosheet as an Efficient Trap for the Permanent Sequestration of Vaporâ€Phase Elemental Mercury. Advanced Science, 2019, 6, 1901410.	11.2	57
56	Role of flue gas components in HgO oxidation over La0.8Ce0.2MnO3 perovskite catalyst in coal combustion flue gas. Chemical Engineering Journal, 2019, 360, 1656-1666.	12.7	56
57	Porous extruded-spheronized Li4SiO4 pellets for cyclic CO2 capture. Fuel, 2019, 236, 1043-1049.	6.4	54
58	Selenide functionalized natural mineral sulfides as efficient sorbents for elemental mercury capture from coal combustion flue gas. Chemical Engineering Journal, 2020, 398, 125611.	12.7	53
59	An overview of sulfur-functional groups in biochar from pyrolysis of biomass. Journal of Environmental Chemical Engineering, 2022, 10, 107185.	6.7	53
60	Dual Roles of Nano-Sulfide in Efficient Removal of Elemental Mercury from Coal Combustion Flue Gas within a Wide Temperature Range. Environmental Science & Technology, 2018, 52, 12926-12933.	10.0	52
61	Density Functional Theory Study of Mercury Adsorption on CuS Surface: Effect of Typical Flue Gas Components. Energy & Fuels, 2019, 33, 1540-1546.	5.1	51
62	Advances in flue gas mercury abatement by mineral chalcogenides. Chemical Engineering Journal, 2021, 411, 128608.	12.7	51
63	Valorization of the aqueous phase produced from wet and dry thermochemical processing biomass: A review. Journal of Cleaner Production, 2021, 294, 126238.	9.3	48
64	Coexistence of enhanced Hg0 oxidation and induced Hg2+ reduction on CuO/TiO2 catalyst in the presence of NO and NH3. Chemical Engineering Journal, 2017, 330, 1248-1254.	12.7	47
65	Preparation of spherical Li4SiO4 pellets by novel agar method for high-temperature CO2 capture. Chemical Engineering Journal, 2020, 380, 122538.	12.7	47
66	Development of selenized magnetite (Fe3O4â~'xSey) as an efficient and recyclable trap for elemental mercury sequestration from coal combustion flue gas. Chemical Engineering Journal, 2020, 394, 125022.	12.7	47
67	Charge distribution modulation and morphology controlling of copper selenide for an enhanced elemental mercury adsorption activity in flue gas. Chemical Engineering Journal, 2022, 442, 136145.	12.7	47
68	Enhanced activity of AgMgOTiO2 catalyst for photocatalytic conversion of CO2 and H2O into CH4. International Journal of Hydrogen Energy, 2016, 41, 8479-8488.	7.1	45
69	Role of SO2 and H2O in the mercury adsorption on ceria surface: A DFT study. Fuel, 2020, 260, 116289.	6.4	45
70	Removal of flue gas mercury by porous carbons derived from one-pot carbonization and activation of wood sawdust in a molten salt medium. Journal of Hazardous Materials, 2022, 424, 127336.	12.4	44
71	NH3 inhibits mercury oxidation over low-temperature MnOx/TiO2 SCR catalyst. Fuel Processing Technology, 2018, 176, 124-130.	7.2	39
72	Machine learning aided bio-oil production with high energy recovery and low nitrogen content from hydrothermal liquefaction of biomass with experiment verification. Chemical Engineering Journal, 2021, 425, 130649.	12.7	38

#	Article	IF	CITATIONS
73	Simultaneous NO Reduction and Hg <sup>0</sup> Oxidation over La <sub>0.8</sub> Ce <sub>0.2</sub> MnO <sub>3</sub> Perovskite Catalysts at Low Temperature. Industrial & Engineering Chemistry Research, 2018, 57, 9374-9385.	3.7	37
74	Recyclable chalcopyrite sorbent for mercury removal from coal combustion flue gas. Fuel, 2021, 290, 120049.	6.4	36
75	Coordinatively Unsaturated Selenides over CuFeSe <sub>2</sub> toward Highly Efficient Mercury Immobilization. Environmental Science & Technology, 2022, 56, 575-584.	10.0	36
76	Cold Flow Properties of Biodiesel and the Improvement Methods: A Review. Energy & Fuels, 2020, 34, 10364-10383.	5.1	35
77	Facile preparation of nanosized copper sulfide functionalized macroporous skeleton for efficient vapor-phase mercury sequestration. Chemical Engineering Journal, 2021, 419, 129561.	12.7	33
78	Stability of mercury on a novel mineral sulfide sorbent used for efficient mercury removal from coal combustion flue gas. Environmental Science and Pollution Research, 2018, 25, 28583-28593.	5.3	32
79	Amorphous molybdenum selenide intercalated magnetite as a recyclable trap for the effective sequestration of elemental mercury. Journal of Materials Chemistry A, 2020, 8, 14955-14965.	10.3	30
80	Machine learning predicting wastewater properties of the aqueous phase derived from hydrothermal treatment of biomass. Bioresource Technology, 2022, 358, 127348.	9.6	29
81	Nanosized Copper Selenide for Mercury Removal from Indoor Air and Emergency Disposal of Liquid Mercury Leakage. Industrial & Engineering Chemistry Research, 2019, 58, 21881-21889.	3.7	28
82	Effect of sulfite on divalent mercury reduction and re-emission in a simulated desulfurization aqueous solution. Fuel Processing Technology, 2017, 165, 138-144.	7.2	27
83	Toward an Understanding of Fundamentals Governing the Elemental Mercury Sequestration by Metal Chalcogenides. Environmental Science & Technology, 2020, 54, 9672-9680.	10.0	27
84	The adsorption mechanisms of HgO on marcasite-type metal selenides: The influences of metal-terminated site. Chemical Engineering Journal, 2021, 406, 126723.	12.7	27
85	Synergistic effect of HCl and NO in elemental mercury catalytic oxidation over La2O3-TiO2 catalyst. Fuel, 2018, 215, 232-238.	6.4	26
86	High-temperature CO2 capture by Li4SiO4 adsorbents: Effects of pyroligneous acid (PA) modification and existence of CO2 at desorption stage. Fuel Processing Technology, 2020, 197, 106186.	7.2	26
87	Performance and Mechanism of Potassium Ferrate(VI) Enhancing Dark Fermentative Hydrogen Accumulation from Waste Activated Sludge. ACS Sustainable Chemistry and Engineering, 2020, 8, 8681-8691.	6.7	25
88	Theoretical prediction the removal of mercury from flue gas by MOFs. Fuel, 2016, 184, 474-480.	6.4	24
89	Elemental Mercury Removal from Flue Gas over TiO <sub>2</sub> Catalyst in an Internal-Illuminated Honeycomb Photoreactor. Industrial & Engineering Chemistry Research, 2018, 57, 17348-17355.	3.7	23
90	Adsorption and Oxidation of Elemental Mercury on Chlorinated ZnS Surface. Energy & Fuels, 2018, 32, 7745-7751.	5.1	22

#	Article	IF	CITATIONS
91	Density Functional Theory Study of Elemental Mercury Immobilization on CuSe(001) Surface: Reaction Pathway and Effect of Typical Flue Gas Components. Industrial & Engineering Chemistry Research, 2020, 59, 13603-13612.	3.7	20
92	Reduction of polycyclic aromatic hydrocarbons (PAHs) emission from household coal combustion using ferroferric oxide as a coal burning additive. Chemosphere, 2020, 252, 126489.	8.2	18
93	Single step fabrication of spherical CaO pellets via novel agar-assisted moulding technique for high-temperature CO2 capture. Chemical Engineering Journal, 2021, 404, 127137.	12.7	18
94	The influences of selenium species on mercury removal over pyrite surface: A density functional theory study. Fuel, 2021, 292, 120284.	6.4	17
95	Favorably adjusting the pore characteristics of copper sulfide by template regulation for vapor-phase elemental mercury immobilization. Journal of Materials Chemistry A, 2022, 10, 10729-10737.	10.3	17
96	Density Functional Theory Studies of the Adsorption and Interactions between Selenium Species and Mercury on Activated Carbon. Energy & Fuels, 2020, 34, 9779-9786.	5.1	16
97	Thermochemical Energy Storage of Concentrated Solar Power by Novel Y <sub>2</sub> O <sub>3</sub> -Doped CaO Pellets. Energy & Fuels, 2021, 35, 12610-12618.	5.1	16
98	Theoretical Study on Hg <sup>0</sup> Adsorption and Oxidation Mechanisms over CuCl <sub>2</sub> -Impregnated Carbonaceous Material Surface. Energy & Fuels, 2018, 32, 7125-7131.	5.1	13
99	Synthesis of Activated Carbon from Citric Acid Residue by Phosphoric Acid Activation for the Removal of Chemical Oxygen Demand from Sugar-Containing Wastewater. Environmental Engineering Science, 2019, 36, 656-666.	1.6	13
100	Porous spherical calcium aluminate-supported CaO-based pellets manufactured via biomass-templated extrusion–spheronization technique for cyclic CO2 capture. Environmental Science and Pollution Research, 2019, 26, 21972-21982.	5.3	13
101	Advances in magnetically recyclable remediators for elemental mercury degradation in coal combustion flue gas. Journal of Materials Chemistry A, 2020, 8, 18624-18650.	10.3	10
102	Reduction of oxidized mercury over NOx selective catalytic reduction catalysts: A review. Chemical Engineering Journal, 2021, 421, 127745.	12.7	10
103	Binary mineral sulfides sorbent with wide temperature range for rapid elemental mercury uptake from coal combustion flue gas. Environmental Technology (United Kingdom), 2021, 42, 160-169.	2.2	10
104	The impact of the particle size of meat and bone meal (MBM) incineration ash on phosphate precipitation and phosphorus recovery. Journal of Environmental Chemical Engineering, 2021, 9, 105247.	6.7	9
105	Light irradiation inhibits mercury adsorption by mineral sulfide sorbent. Fuel, 2021, 288, 119663.	6.4	8
106	Numerical simulation of sorbent injection for mercury removal within an electrostatic precipitator: In-flight plus wall-bounded mechanism. Fuel, 2022, 309, 122142.	6.4	8
107	Mechanisms of Gas-Phase Mercury Immobilized by Metal Sulfides from Combustion Flue Gas: A Mini Review. Energy & Fuels, 2022, 36, 6027-6037.	5.1	8
108	Li4SiO4 pellets templated by rice husk for cyclic CO2 capture: Insight into the modification mechanism. Ceramics International, 2021, 47, 32060-32067.	4.8	7

#	Article	IF	CITATIONS
109	HgCl <sub>2</sub> Reduction under a Low-Temperature Selective Catalytic Reduction Atmosphere. Energy & Fuels, 2020, 34, 2417-2424.	5.1	6
110	A Molten-Salt Pyrolysis Synthesis Strategy toward Sulfur-Functionalized Carbon for Elemental Mercury Removal from Coal-Combustion Flue Gas. Energies, 2022, 15, 1840.	3.1	6
111	Facile pathway towards crystallinity adjustment and performance enhancement of copper selenide for vapor-phase elemental mercury sequestration. Chemical Engineering Journal, 2022, 430, 132811.	12.7	5
112	Efficient reduction of CO 2 to CO by Ag 3 PO 4 /TiO 2 photocatalyst under ultraviolet and visible light irradiation. Asia-Pacific Journal of Chemical Engineering, 2020, 15, e2499.	1.5	4
113	Comprehensive investigation into in-situ chemical oxidation of ferrous iron/sodium percarbonate (Fe(II)/SPC) processing dredged sediments for positive feedback of solid–liquid separation. Chemical Engineering Journal, 2021, 425, 130467.	12.7	4
114	Trace element partition in coal fires. , 2019, , 105-142.		2